



Contents lists available at ScienceDirect

Gynecologic Oncology

journal homepage: www.elsevier.com/locate/ygyno

Evaluation of the first Ergocalciferol-derived, non hypercalcemic anti-cancer agent MT19c in ovarian cancer SKOV-3 cell lines

Laurent Brard ^{a,1,2}, Thilo S. Lange ^{a,b,2}, Katina Robison ^a, Kyu Kwang Kim ^a, Tahniyath Ara ^c, Megan Marie McCallum ^c, Leggy A. Arnold ^c, Richard G. Moore ^a, Rakesh K. Singh ^{a,*}

^a Molecular Therapeutics Laboratory, Program in Women's Oncology, Department of Obstetrics and Gynecology, Women and Infants' Hospital, Alpert Medical School, Brown University, Providence, RI 02905, USA

^b Molecular Biology, Cell Biology, and Biochemistry, Brown University, Providence, RI 02912, USA

^c Chemistry and Biochemistry, University of Wisconsin-Milwaukee, Milwaukee, WI 53551, USA

ARTICLE INFO

Article history:

Received 20 April 2011

Available online xxxxx

Keywords:

Vitamin-d

Calcitriol

MT19c

Hypercalcemia

Apoptosis

VDR

ABSTRACT

Objective. In human trials calcitriol and its analogs displayed unacceptable systemic toxicities including hypercalcemia. This study was designed to evaluate a novel non-hypercalcemic vitamin-D derivative (MT19c) and its anticancer effects in cultured ovarian cancer cell model.

Methods. We modified the Ergocalciferol structure to generate MT19c, a heterocyclic vitamin-D derivative. Hypercalcemic liabilities of MT19c were assessed by estimating the blood calcium levels in drug treated animals. VDR agonistic or antagonistic properties of MT19c were determined via a VDR-coactivator binding assay. The anticancer effects of MT19c were evaluated by (i) cytotoxicity studies in cancer cell lines and the National Cancer Institute (NCI₆₀) cell lines, (ii) identification of apoptosis markers by microscopy and western blots, (iii) cell cycle analysis, and (iv) by studying the insulin receptor substrate-1/2 (IRS1/2) signaling in ovarian cancer cells (SKOV-3) by western blotting.

Results. MT19c treatment did not cause hypercalcemia in mice and showed minor VDR antagonistic activity. In a NCI₆₀ screen MT19c revealed cell-type specific growth inhibition. MT19c displayed superior cytotoxicity to cisplatin, calcitriol, EB1089 and Iressa in SKOV-3 cell-lines and was comparable to Taxol in our *in vitro* assays. In SKOV-3 cells MT19c showed caspase dependent apoptosis, DNA fragmentation and cell cycle arrest. MT19c did not alter VDR but downregulated the IGF1R/IRS-1/2-MEK-ras-ERK1/2-pathway via activated TNF α -receptor/SAPK/JNK component.

Conclusion. Our results demonstrate how structural optimization of the vitamin-D scaffold leads to identification of a non-hypercalcemic compound MT19c which exerts cytotoxicity *in vitro* based on a VDR-independent signaling pathway and displays potent anti-cancer activity in ovarian cancer cell models.

© 2011 Elsevier Inc. All rights reserved.

Introduction

Epithelial ovarian cancer (EOC) is the leading cause of death from gynecologic malignancies [1]. Although most patients respond to cytoreductive surgery followed by adjuvant platinum-based chemotherapy the majority will experience disease recurrence and resistance to most chemotherapeutic agents [2]. The majority of women diagnosed with ovarian cancer in advanced stage have a low survival rate pressing the need for more effective therapies and or treatment approaches [2].

The Vitamin-D receptor (VDR) ligands Calcitriol and EB1089 have been shown to have anti-cancer effects in various *in vitro* and animal models of prostate, ovarian, pancreatic, skin, colon, leukemia and breast cancer [3,4]. Calcitriol and EB1089 cause induction of differentiation, inhibition of proliferation, and modulation of cell cycle progression and suppression of invasiveness, induction of metastasis, and angiogenesis including caspase dependent or independent apoptosis [3–5]. Phase 2 clinical trials that evaluated the use of calcitriol and EB1089 in patients with prostate, breast, colorectal, leukemia, ovarian and pancreatic cancers identified dose-limiting hypercalcemia and other grade 3/4 toxicities that limit the clinical utility of these drugs [3–5].

The development of calcitriol/vitamin D3 analogs with decreased hypercalcemic effects has emerged as an important strategy for cancer treatment including ovarian cancer [3,4]. To reduce the hypercalcemic effects of calcitriol complex chemical manipulations of its core scaffold have been carried out to identify structure-activity relationships that can lead to reduced hypercalcemia but improved anticancer effects [3]. However hypercalcemia continues to be the persistent

* Corresponding author at: Program in Women's Oncology, Department of Obstetrics and Gynecology, Women and Infants Hospital of RI, 101 Dudley Street, Providence, RI 02905, USA. Fax: +1 401 277 3617.

E-mail address: rsingh@wilhi.org (R.K. Singh).

¹ Present Address: Division of Gynecologic Oncology, Department of Obstetrics and Gynecology, Southern Illinois University School of Medicine, Springfield, IL 62794, USA.

² These authors contributed equally to the manuscript.

problem associated with modified VDR ligands. We designed a triazolinedione adduct of Ergocalciferol with a N-substituted-1,2,4-triazolinedione which was further converted to the corresponding bromoacetate derivative MT19c [6]. MT19c is a conformationally constrained heterocyclic vitamin-D analog derived as opposed to the carbonaceous Calcitriol. Heteroatoms in the MT19c A-ring were incorporated to improve the toxicity and drug-like characteristics of MT19c and to disable 1- α -hydroxylase catabolism that is linked to genomic VDR signaling and hypercalcemia. In the current study, we evaluated the anticancer efficacy of MT19c via *in vitro* experiments using the ovarian cancer cell line SKOV-3 and determined its hypercalcemic effects in animals. VDR receptor interactions of MT19c were assessed by a fluorescence polarization assay.

Methods

Synthesis of MT19c

Details for the synthesis and structural characterization of MT19c using NMR (^1H), Mass spectrometry, and X-ray crystallography are described in the Supplementary Information section (S-1). Briefly, commercially available Ergocalciferol underwent a Diels-Alder reaction with N-methyl-1,2,4-triazolinedione to synthesize intermediate adduct (Fig. 1A; structure 2), which upon reaction with bromoacetic acid in presence of DCC (N,N'-dicyclohexylcarbodiimide) generated MT19c (Fig. 1A) in good yield [6]. The crystal structure of MT19c is shown in the Fig. 1B.

Reagents and cell culture

Human ovarian epithelial adenocarcinoma cell line SKOV-3, human pancreatic adenocarcinoma BxPC-3, human prostate adenocarcinoma

PC-3 and LNCaP, human neuroblastoma SH-SY5Y and SK-N-SH cell lines were obtained from American Type Culture Collection ATCC (Manassas, VA, USA). SMS-KCNR (human neuroblastoma) cells were provided by Dr. Giselle Sholler (University of Vermont). Human umbilical vein endothelial cells (HUVECs) were obtained from Lonza Inc. (Allendale, NJ). All cells were seeded at 5×10^5 /T75 flask (Corning, NY, USA) and cultured to ~80% confluency according to the suppliers' recommendations. Calcitriol (Alexis Corporation, CA, USA), Cisplatin, Paclitaxel (Sigma-Aldrich, Saint-Louis, MO, USA) and ZD1839 (LC Laboratories, Woburn, MA, USA) were purchased. EB1089 (Leo Pharmaceuticals; Ballerup, Denmark) was kindly provided by the manufacturer. Recombinant insulin-like growth factor-1 (IGF1) and tumor necrosis factor (TNF) were purchased from R&D systems (Minneapolis, MN, USA), and insulin was purchased from Sigma-Aldrich (Saint Louis, MO, USA). For all assays cells were seeded in complete DMEM media and allowed to attach overnight.

Cell viability assay

Viability of MT19c (0–10 μM) or vehicle treated cells was determined by a 96 s Aqueous-One-Solution Assay (Promega, Madison, WI, USA). The assay was carried out as described previously [7] with incubation periods as indicated. Experiments were performed in triplicates; data are expressed as the mean of the triplicate determinations ($X \pm \text{SD}$) of a representative experiment in % of absorbance by samples with untreated cells (= 100%).

NCI 60 cancer cell-line assay

MT19c was screened through the National Cancer Institute (NCI) Developmental Therapeutics Program (DTP) 60 human cancer cell-line panel under the *in vitro* Cell-line screening Project (IVCLSP) (www.dtp).

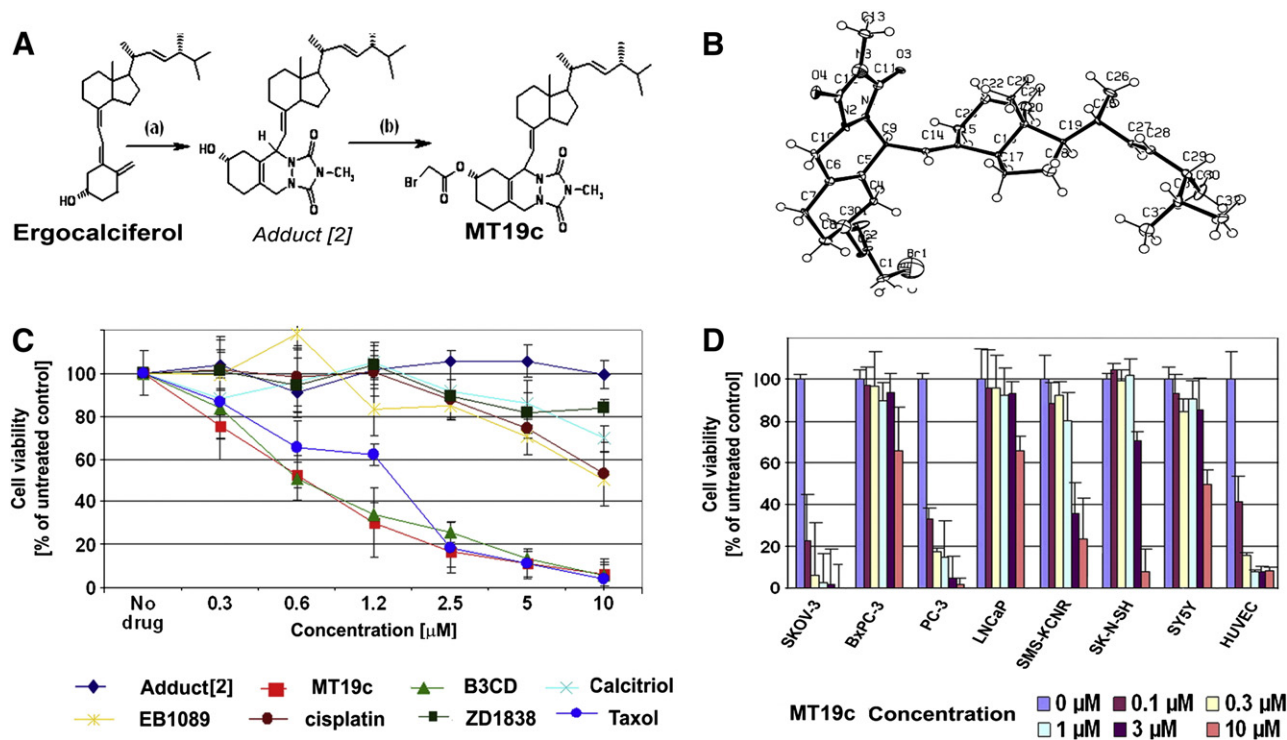


Fig. 1. Synthesis and comparative analysis of MT19c cytotoxicity *in vitro*. (A) Scheme of MT19c synthesis. (a): 4-methyl-1,2,4-triazolone-3,5-dione, EtOAc, 0 °C, 2 h, N₂; (b): Bromoacetic acid, 1,3-dicyclohexylcarbodiimide, anhydrous DCM, 0 °C–RT, 4 h, N₂. (B) Crystal structure of MT19c (C) Cytotoxic effect of MT19c versus calcitriol/vitamin-D3 and analogs/derivatives, cisplatin, Iressa, and Paclitaxel in an EOC cell-line. SKOV-3 cells were treated with of MT19c, its precursor (adduct [2]), calcitriol/vitamin-D3, EB1089, B3CD and controls (cisplatin, Iressa/ZD1839, Paclitaxel) for 24 h and a viability assay carried out. Three independent experiments were performed. Data are expressed as means of triplicate determinations ($X \pm \text{SD}$) of a representative experiment in % cell viability of untreated cells (= 100%) (D) Cytotoxic effects of MT19c in various human cancer cell lines. SKOV-3, BxPC-3 (pancreatic cancer), PC-3 and LNCaP (prostate cancer), SMS-KCNR, SK-N-SH and SH-SY5Y (neuroblastoma), as well as HUVEC (endothelial) were treated with MT19c (0–10 μM) for 48 h. Three independent experiments were performed. Data are expressed as means of triplicate determinations ($X \pm \text{SD}$) of a representative experiment in % cell viability of untreated cells (= 100%).

nci.nih.gov). The details of the method and the repeat screening results are shown in Supplementary Information section (S-2).

Estimation of blood calcium levels (hypercalcemia) in mice

All animal experiments were performed in the animal facilities of Rhode Island Hospital (RIH) with strict adherence to the guidelines of the Animal Welfare Committee of RIH and Women & Infants Hospital (AWC protocol #0185-06) in accordance with the guidelines set by the NIH in the care and use of laboratory animals. Thirteen six-week old female nude mice (nu/nu strain code 088/homozygous, 25 g average weight) (Charles River Laboratories, MA, USA) were randomly assigned to a control group (4 animals) or treatment group (9 animals). Vehicle (PBS/2.5% EtOH) or MT19c at 5 mg/kg bwt MT19c in 0.3 ml of vehicle was administered intraperitoneally (IP) every other day for 90 days. Serum calcium levels were taken from the saphenous vein on day 40 and cardiac puncture was performed on day 90 (endpoint). Calcium concentration analysis was performed by IDEXX Laboratories Inc. (North Grafton, MA).

Determination of agonistic/antagonistic properties of MT19c using a VDR-coactivator binding assay

The assay has been described in detail previously [8]. Briefly, MT19c was serially diluted in DMSO and 100 nl of each concentration was transferred into 20 μ L protein buffer 7.5 nM SRC2-3 (CKKKENALLRYLLDKDDTKD) labeled with Alexa Fluor® 647 Maleimide, and 1 μ M VDR-LBD in the presence and absence of Calcitriol (100 nM) in quadruplet using black 384 well plate (Costar, Cat No-3658). The samples were allowed to equilibrate for 2 h. Binding was then measured using fluorescence polarization (excitation 620 nm, emission 688 nm) using a M1000 plate reader (Tecan). The experiments were evaluated using GraphPad Prism 5, and IC₅₀ values were obtained by fitting the data to an equation (Sigmoidal dose–response-variable slope (four parameters)). Values are given as the mean values with a 95% confidence interval. For the antagonist assay CBT1 (20 μ M) and DMSO, and for the agonist assay Calcitriol 100 nM and DMSO were used as positive and negative control, respectively.

Cell proliferation assay

Cell proliferation was determined by a BrdU assay (Roche Applied Science, Indianapolis, IN, USA) measuring the incorporation of the 5-bromo-20-deoxyuridine (BrdU) during DNA synthesis. Briefly, cells (5×10^3) were seeded into 96-well plates (Corning Incorporated, USA) and allowed to attach overnight before treatment with MT19c (0–2 μ M) for 24 h in complete medium. The assay was carried out and analyzed as described previously [7].

Morphological studies

SKOV-3 cells were seeded (1×10^4 /chamber) into a Lab-Tek Chamber-Slide System (Nalge Nunc., Naperville, IL) and treated for 24 h with 1 μ M MT19c alongside with non-treated cells. Following two wash steps in PBS the cells were fixed in PBS, 2% PFA, 0.2% Triton X for 20 min at RT and stained for 10 min with 200 ng/ml 4'-6-Diamidino-2-Phenylindole (DAPI) in PBS before mounting. Representative images were taken with an inverted microscope (Nikon Eclipse TE2000-E, CCD camera) and 20 \times objective.

Cell cycle analysis (by FACS)

SKOV-3 cells were seeded into 100 mm² tissue culture dishes (1×10^6 cells/dish) (Corning Inc., NY) in complete DMEM media, treated with vehicle, or MT19c (500 nM) for 12 or 18 h, and the assay carried

out as described previously [7]. Appropriate gating was used to select single cell population. Experiments were performed in duplicate.

Western blot analysis

SKOV-3 cells were seeded into 6-well plates (3×10^5 cells/dish) before treatment with MT19c (1 μ M). Preparation of cell lysates, PAGE and immunoblotting with appropriate antibodies was carried out as described previously [7]. All primary and secondary antibodies were purchased from Cell Signaling technology, Beverly, MA, USA. As a size standard pre-stained Precision Plus Protein Kaleidoscope (BioRad, Hercules, CA, USA) marker was used. The details of the antibodies are provided in the Supplementary Information Section (S-3).

Results

Synthesis and in vitro cytotoxicity of MT19c

We designed a novel heterocyclic derivative of Ergocalciferol named MT19c. We characterized the structure of MT19c by NMR, Mass spectrometry and X-ray crystallography (Fig. 1B). To analyze the effects of MT19c in comparison to its precursor (adduct [2]), Calcitriol or analog B3CD, Taxol and two other cytotoxic agents, ZD1839 (Iressa) and Cisplatin, we performed a viability assay in a human platinum-resistant EOC cell line (SKOV-3). Cells were treated for 24 h with 0.3–10 μ M of drug or vehicle. MT19c revealed cytotoxicity in the nanomolar range (IC₅₀ ~500–600 nM) (Fig. 1C). MT19c effects were superior to calcitriol, EB1089, ZD1838 and Cisplatin. MT19c potency in SKOV-3 cells was comparable to Taxol and B3CD (Fig. 1C).

MT19c (100–300 nM) proved to be highly cytotoxic to SKOV-3 and PC-3 (prostate adenocarcinoma) cancer cells as well as HUVEC (human umbilical vein endothelial cells) but not to BxPC3 (pancreatic adenocarcinoma), LNCaP (prostate adenocarcinoma) or various neuroblastoma cell lines (SH-SY5Y, SK-N-SH, SMS-KCNR) (Fig. 1D). Broader cytotoxic effects and comparison of GI₅₀, TGI, and LC₅₀ revealed cell-type or tumor-type specificity in the effectiveness of MT19c against chemoresistant cancer cell lines derived from nine different tissue-types in a NCI₆₀ cell-line screen (Fig. 2) (<http://dtp.nci.nih.gov/>).

Effects of MT19c on serum calcium levels in animals

Currently known calcitriol analogs cause hypercalcemia. We investigated if MT19c treatment caused hypercalcemia in animals despite the structural modification of Ergocalciferol discussed above. In animals, MT19c did not cause hypercalcemia at the dose tested. Serum calcium levels in MT19c treated mice (5 mg/kg bwt) did not significantly differ from the control group ($p=0.8$) (Fig. 3A). In the treatment group the mean serum calcium level was 8.96 mg/dl on day 40 and 10.02 mg/dl on day 90. In the control group the mean serum calcium level was 10.0 mg/dl on day 40 and 11.13 mg/dl on day 90 (Fig. 3A). MT19c is $\sim 5 \times 10^6$ times less hypercalcemic than Calcitriol [9,10], and $\sim 10^4$ times less hypercalcemic than EB1089.

MT19c is a weak VDR antagonist

The biochemical interactions between MT19c and VDR were investigated using a fluorescence polarization assay [8]. MT19c was incubated with VDR-LBD and a fluorescent labeled coactivator peptide (SRC2-3) in the presence and absence of calcitriol. In the presence of calcitriol, VDR is able to interact with the coactivator peptide SRC2-3. VDR antagonists are able to disrupt this interaction by a direct or allosteric mode of inhibition. MT19c showed a very weak antagonistic effect at a concentration of 15 μ M and higher (Fig. 3B). Full inhibition was not reached even at a concentration of 1 mM. The ability of MT19c to bind to VDR and initiate the conformational change of VDR to allow

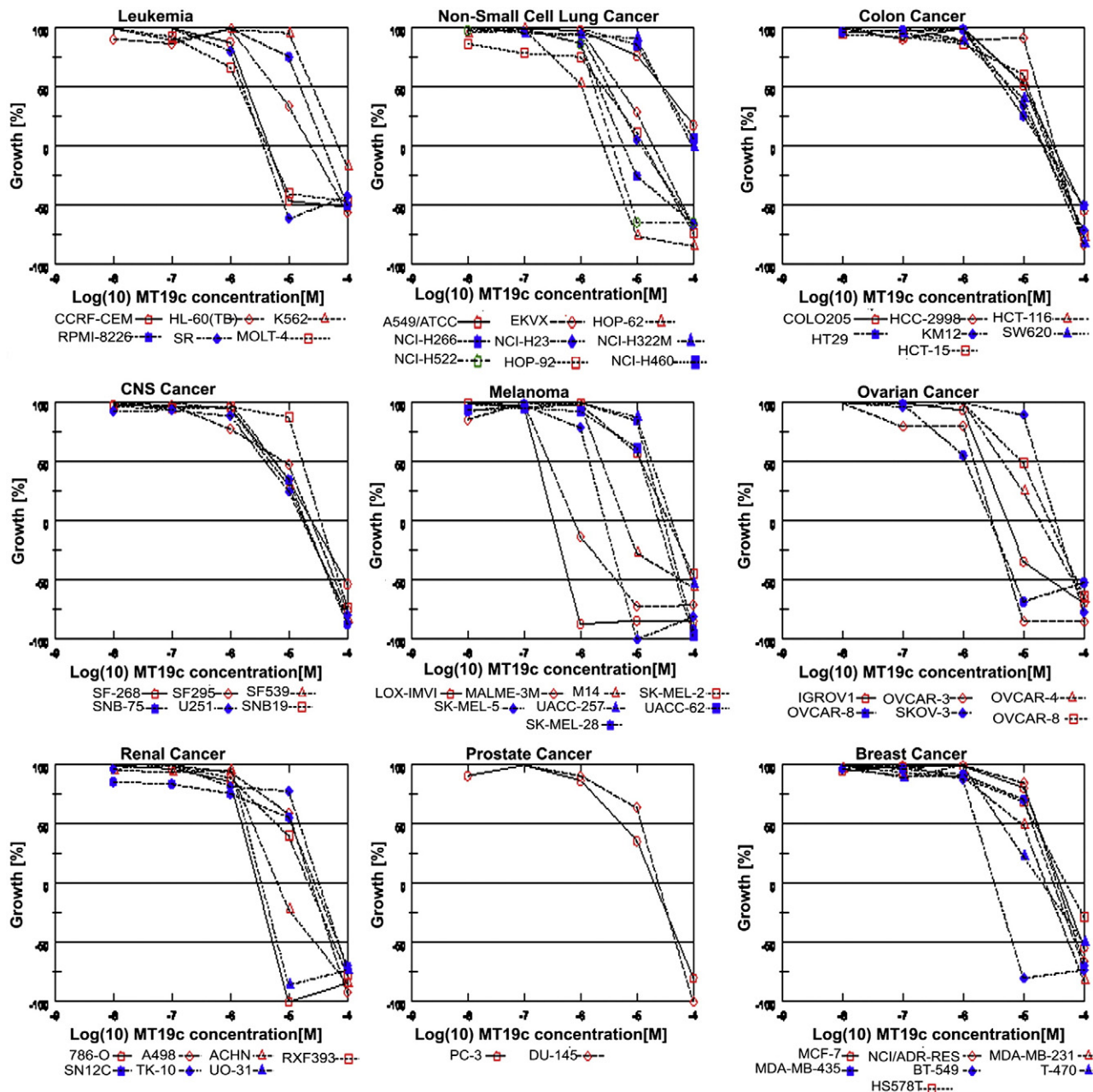


Fig. 2. Cytotoxic properties of MT19c in NCI60 cell line panel. Growth Inhibitory (GI50), Total Growth Inhibition (TGI) or Lethal concentration (LC50) of MT19c against a panel of 60 chemoresistant cancer cell lines derived from leukemia, non small cell lung cancer cell, colon, CNS, melanoma, ovarian cancer, renal, prostate and breast cancer was determined in a National Cancer Institute (NCI) run screen (<http://dtp.nci.nih.gov/>).

coactivator recruitment was determined in the absence of calcitriol. Our results clearly show that MT19c is not a VDR agonist (Fig. 3B). Similarly, MT19c treated SKOV-3 cells did not show any change in the expression of VDR (Fig. 3C).

Induction of apoptosis and activation of MAPKs in SKOV-3 cells after MT19c treatment

To understand the cellular mechanisms involved in the response to MT19c we examined the cellular structure and intracellular bodies of SKOV-3 cells by microscopy. Cells treated for 24 h with 1 μ M MT19c and after chromatin staining with DAPI displayed densely stained nuclear granular bodies of highly condensed chromatin (Fig. 4A) and TUNEL positive cell (Fig. 4B). Together, these data show that MT19c induces apoptosis in SKOV-3 cells. MT19c (1 μ M) treatment of SKOV-3 cells resulted in the activation/cleavage of initiator caspase-9 and

executioner caspase-3 (Fig. 4C) within 1–4 h while reaching maximal activation within 18 h. Drug exposure resulted in the cleavage of PARP-1 (Fig. 4C) crucial for DNA repair and PARP-1 deactivation serves as an additional marker of cells undergoing apoptosis [11].

Activation of MAP Kinases, suppression of cell proliferation and cell-cycle progression of SKOV-3 cells upon MT19c treatment

Immunoblotting of PAGE-separated cellular lysates revealed that MT19c (1 μ M) caused strong activation of p38 and SAPK/JNK MAPK (Fig. 5A) with a concomitant ERK 1/2 downregulation. The basal level of inactive p38 and ERK 1/2 remained unchanged. MT19c dose-dependently reduced SKOV-3 proliferation (Fig. 5B). At a drug concentration of 500 nM (for 24 h) proliferation of treated SKOV-3 was inhibited by 80% and at 120 nM by 69% as compared to untreated cells. Even at a drug concentration of 60 nM BrdU incorporation into

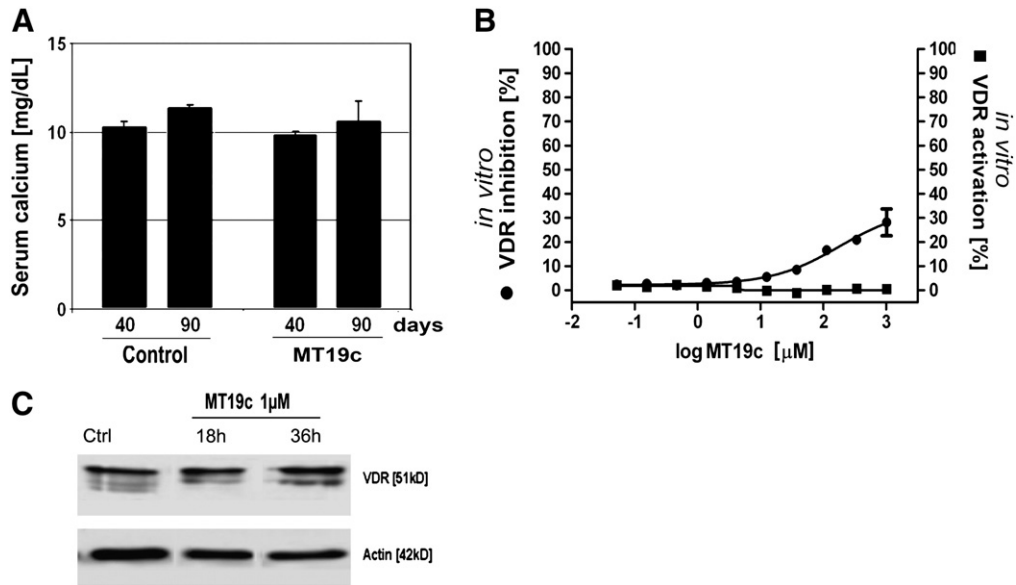


Fig. 3. Non-hypercalcemia in animals and effect of MT19c on vitamin D receptor (VDR) expression. (A) Serum calcium levels in mice after MT19c treatment. Nine mice each were treated with MT19c and four were treated with vehicle for 90 days, blood collected and serum calcium analyzed at day 40 and day 90. Change in mean serum calcium was compared between groups by Student's *T*-test with unequal variances. (B) VDR-coactivator binding assay to determine agonist and antagonist properties of MT19c. VDR-LBD and fluorescently labeled coactivator peptide SRC2-3 was treated with different concentrations of MT19c in the presence (●) (% inhibition) and absence (■) (% activation) of calcitriol (100 nM). Data was determined using fluorescence polarization and normalized to calcitriol (100% activation), CBT1 (Ref-35) (100% inhibition), and vehicle DMSO. (C) VDR-expression in EOC cells after MT19c treatment. SKOV-3 cells were treated with 1 μ M MT19c for 18 or 36 h. Western Blot analysis of cell lysates was carried out in two independent experiments using primary antibodies against VDR. A representative experiment is shown. As an internal standard for equal loading (50 μ g total cell protein/lane) blots were probed with an anti- β -actin antibody.

the DNA was reduced (Fig. 5B). Using FACS we analyzed the effect of 0.5 μ M MT19c on cell cycle progression of SKOV-3 cells. When cells were treated with MT19c for 12 and 18 h the S-phase and G2/M phase

populations remained comparable (18% in S, 19.6% in G2/M at 12 h; 16.7% in S, 13.7% in G2/M at 18 h) but a block of cells progressing through the G1-phase (62.0% at 12 h, 70% at 18 h) was observed as

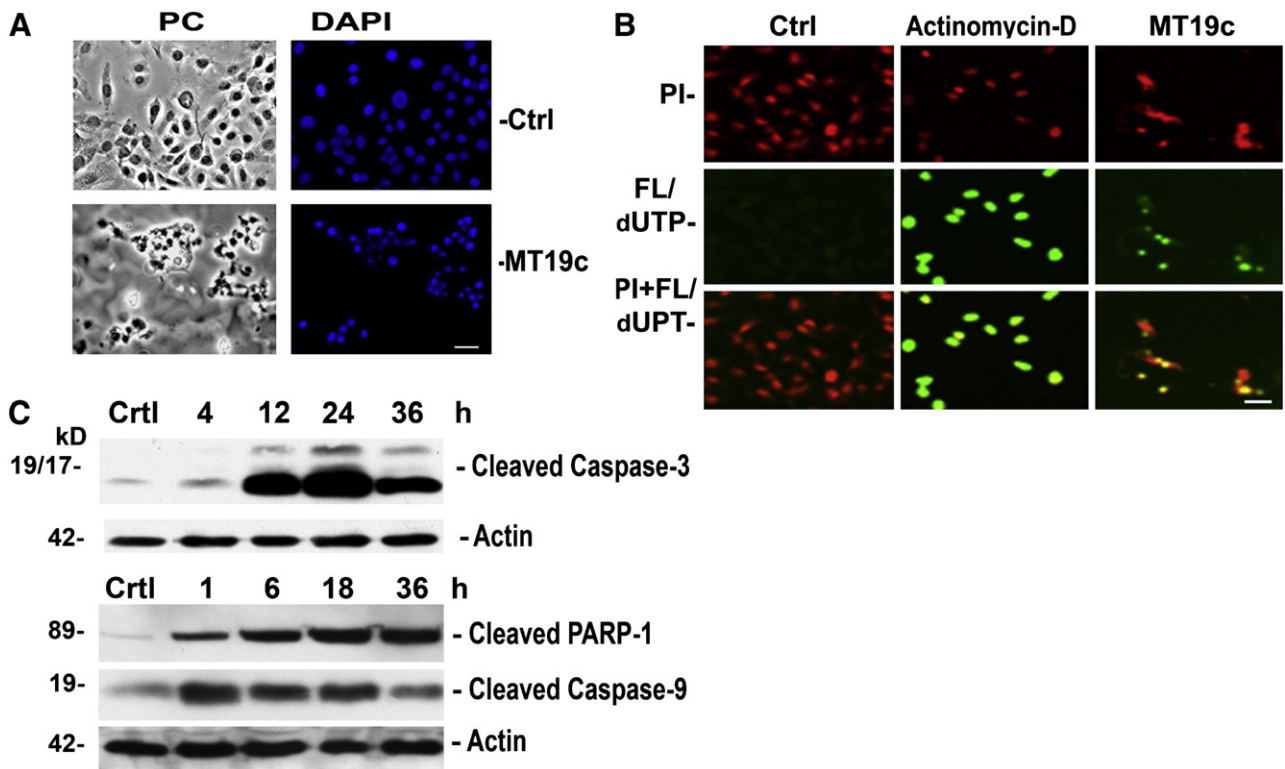


Fig. 4. Cellular and biochemical effects in MT19c treated EOC cells *in vitro*. (A) Morphological appearance/DAPI staining. SKOV-3 cells were treated for 24 h with 1 μ M MT19c before microscopic analysis by phase contrast (PC) or fluorescence analysis after chromatin staining (DAPI) was carried out and repeated twice. Images obtained from a representative experiment are shown. Bar = 10 μ m. (B) Fluorescence microscopy of caspase activation. SKOV-3 cells were treated with 1 μ M MT19c. PAGE and Western blot analysis of cell lysates was carried out in two independent experiments. Activated caspase-3 and -9 and inactivated PARP-1 was visualized by immunoblotting using primary antibodies recognizing cleaved fragments. As an internal standard for equal loading (50 μ g total cell protein/lane) blots were probed with an anti- β -actin antibody. A representative experiment is shown.

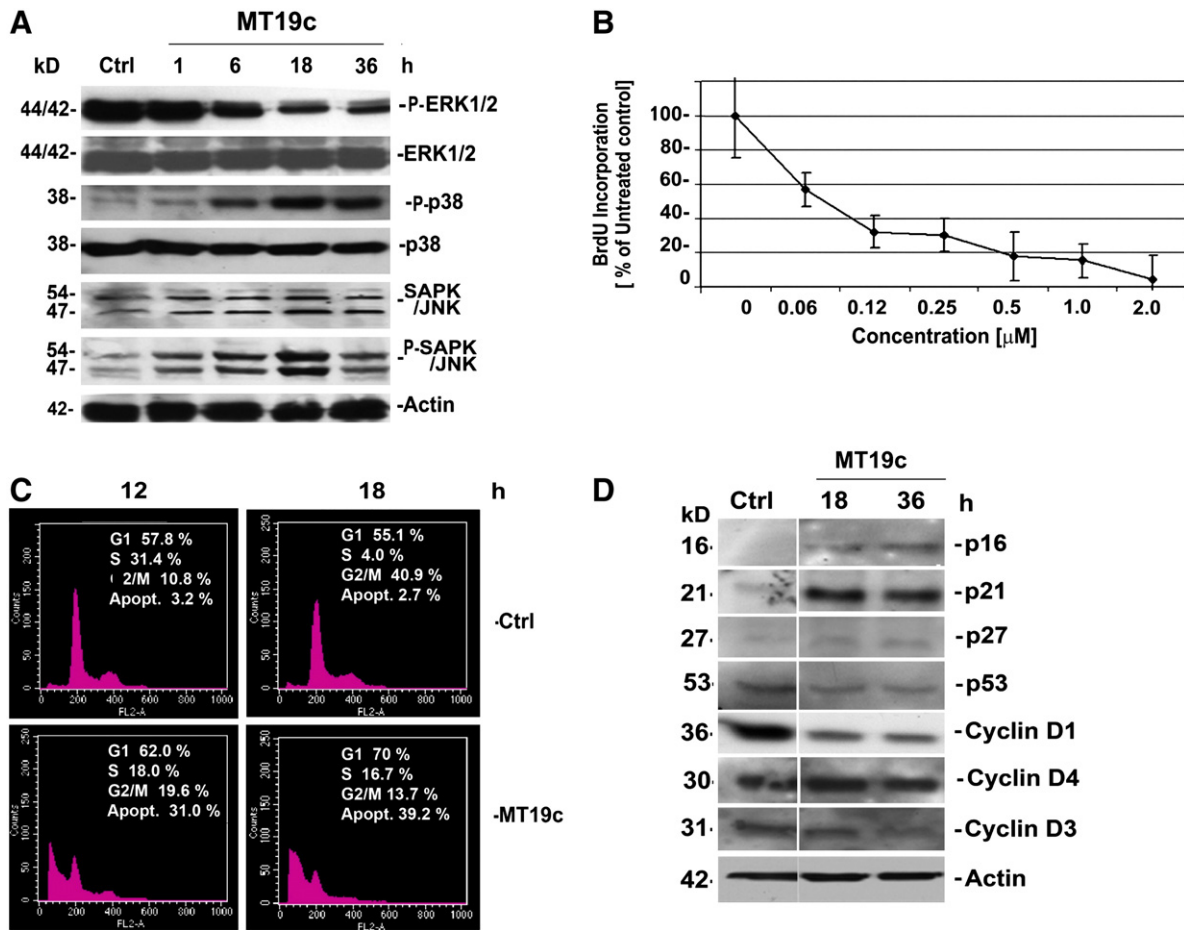


Fig. 5. Activation of MAPKs and cell cycle arrest in SKOV-3 cells upon MT19c treatment. (A) Activation of MAPKs by MT19c in EOC cells. SKOV-3 cells were treated with 1 μ M MT19c or vehicle for 1, 6, 18 or 36 h. PAGE and Western blot analysis of cell lysates was carried out against pro- and activated/phosphorylated (P-) SAP/JNK, p38 and ERK1/2. (B) MT19c inhibits proliferation of EOC cells. SKOV-3 cells were treated with various concentrations (60 nM–2 μ M) of MT19c for 24 h and a colorimetric proliferation assay carried out twice. Data of a representative experiment are expressed as the mean of triplicate determinations ($X \pm SD$) in% of absorbance of treated cells versus untreated cells (= 100%). (C) MT19c causes S-Phase cell cycle arrest in EOC cells. SKOV-3 cells were treated with 500 nM MT19c for 12 or 18 h. Cell cycle analysis by FACS was carried out and repeated twice. Data of a representative experiment are presented as relative fluorescence intensity in a 2-dimensional FACS profile. (D) Expression of cyclin D and cyclin-dependent kinase inhibitors in MT19c EOC cells. Expression of cyclin D1, -D3, -D4, p16, p21, p27 cell cycle regulators and p53 in MT19c (500 nM) and vehicle treated (for 18, 36 h) SKOV-3 cells was analyzed by western blotting. As an internal standard for equal loading (50 μ g total cell protein/lane) blots were probed with an anti- β -actin antibody.

compared to untreated cells (Fig. 5C). The apoptotic populations increased similarly (31.0% at 12 h, 39.2% at 18 h) (Fig. 5C). Western blot analysis of the lysates of SKOV-3 cells upon MT19c (500 nM) treatment caused down-regulation of cyclin-D1, -D3, and -D4 but p16 and p21 were found to be upregulated (Fig. 5D). P21 and p16 proteins are primarily linked to G1-phase regulation [12], the phase in which SKOV-3 cells accumulate following treatment with MT19c.

MT19c inhibits IRS-1/2 signaling in SKOV-3 cells

To determine the pathways that lead to changes in MAPK signaling or are potential targets for the treatment of EOC such as insulin-receptor signaling [13], a western blotting experiment was carried out with SKOV-3 cell lysates after treatment with MT19c (24 h, 1 μ M). Cell treatment with recombinant growth factors IGF (insulin-like growth factor-1), insulin and TNF (tumor necrosis factor) was added as control to the effects observed for MT19c. As shown (Fig. 6A) MT19c, in contrast to IGF-1, insulin, TNF or Calcitriol, deactivated IRS-1 and c-raf. Deactivation of ERK1/2, seen during MT19c treatment, did not occur during IGF-1, insulin or TNF treatment while Calcitriol activated ERK1/2 phosphorylation (Fig. 6A).

Based on these observations we identified the insulin-receptor-substrate (IRS)-1/2 signaling pathway as a target of MT19c. Western blotting against core components of the IRS-1/2 pathway was

performed (Fig. 6B). MT19c reduced expression of IRS-1 and IRS-2 while Calcitriol reduced the expression of IRS-1 but not IRS-2. This down-regulation of inactive IRS-1 was counteracted by IRS-1 activation with Calcitriol, whereas MT19c treatment caused additional IRS-1 inactivation (Figs. 6A and B). In addition, MT19c down-regulated the expression of GRB10 but Calcitriol, IGF and insulin did not (Fig. 6B). To study the effect of MT19c on effectors downstream of IRS-1/2 we performed immunoblotting with antibodies against RSK, MEK, and ELK-1 in addition to c-raf and ERK1/2 (Fig. 6A). RSK was partially deactivated by MT19c and calcitriol but not by insulin or IGF. MEK and ELK-1 were partially deactivated by MT19c but not by calcitriol/vitamin-D3 or insulin or IGF (Fig. 6B) similarly to ERK1/2 (Fig. 6A).

Remarkably, MT19c led to strong activation of SAPK/JNK as opposed to insulin, IGF and Calcitriol. SAPK/JNK is a direct executor of TNFR signaling. Further, we observed up-regulation of TNFR by MT19c (Fig. 6C). The data above support the finding that MT19c cytotoxicity is mediated by suppression of IRS-1/2 signaling in conjunction with TNFR-associated signaling via SAPK/JNK activation.

Discussion

The lack of efficacy and adverse toxicity outcomes of Calcitriol and EB0189 have prompted the development of less hypercalcemic vitamin-D analogs [7,14–17]. The present study outlines the design of a non-

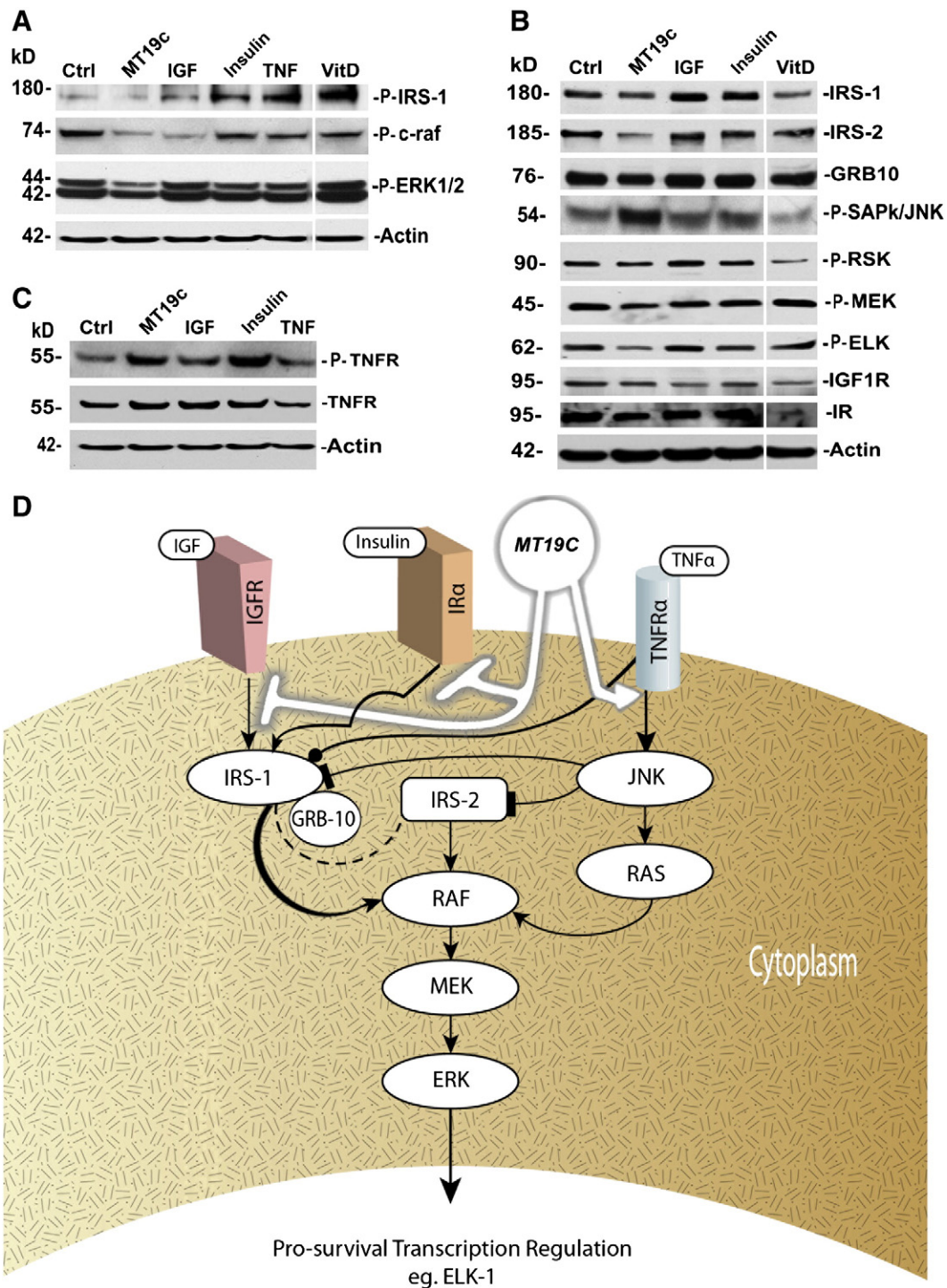


Fig. 6. MT19c effects on the IGF-IRS-MEK-ras-ERK1/2-ELK pathway and on the TNF α receptor in EOC cells. (A–C) Western Blot Analysis of MT19c effects. SKOV-3 cells were treated with 1 μ M MT19c or vehicle for 24 h. Analysis of the expression of proteins by Western blotting of lysates with primary antibodies against pro- and activated/phosphorylated (P-) proteins and receptors associated with IRS-controlled pathways was carried out (Methods). Representative experiments are shown. As an internal standard for equal loading (50 μ g total cell protein/lane) blots were probed with an anti- β -actin antibody. (D) Scheme of MT19c effects on IRS-controlled pathways. MT19c activates TNFR/SAPK/JNK while down-regulating IRS-1 and -2 expression, GRB-10 expression and partially deactivating RSK, c-raf, MEK, ERK1/2 and ELK-1. (\leftarrow activation; T inhibition; \bullet phosphorylation leading to inhibition).

hypercalcemic Vitamin-D analog (MT19c) by modification of the A-ring structure of Ergocalciferol and describes the potent cytotoxic actions of this drug in various *in vitro* anticancer assays and displays lack of hypercalcemia in animals till 90th day of treatment. The structural modification of the A-ring by incorporation of triazolone-dione moiety significantly altered the conformation of carbon (C1) of Ergocalciferol and induced conformational transformation that possibly disabled 1- α -hydroxylase enzyme interaction and therefore resulted in the removal

of hypercalcemic liability in animals. The present study shows that MT19c is the first truly non-hypercalcemic vitamin-D derivative.

By stepwise immunoblotting we identified the IRS-1/2 signaling pathway as a potential target of MT19c (see Model; Fig. 6D). This pathway and its core components [18,19] play a distinct role in cancer onset and progression. The IRS-1/2 pathway is controlled by growth factor receptor signaling (e.g. IGF-1R, IR, TNFR) and IRS are adaptor proteins that link upstream activators to multiple effectors. While IRS-

1 is associated with tumor growth and proliferation, IRS-2 has been linked to tumor-motility and invasion [20–22]. MT19c reduced the expression of IRS-1 and IRS-2. In addition, MT19c down-regulated the expression of GRB10 which inhibits IRS signaling by disrupting the association of IRS-1/IRS-2 with the insulin-receptor [20]. MT19c changed the phosphorylation state of pathway components downstream of IRS-1/2 (e.g., RSK, RAF, MEK and ERK1/2). MT19c partially inactivated RSK, which regulates diverse cellular processes including cancer cell proliferation [23]. MT19c also inactivated c-raf, isoforms of which are known to mediate growth-factor-stimulated growth in EOC cells [24]. MEK inhibition such as seen after MT19c treatment is known to enhance tumor apoptosis in EOC [25]. Finally, MT19c deactivated ERK1/2 (unlike IGF-1, insulin or TNF) while Calcitriol activated ERK1/2 as shown in breast cancer cells [20]. In short, Raf/MEK/ERK signaling, which takes a center stage in malignant transformation and drug resistance, is inhibited by MT19c [24]. Moreover, MT19c suppresses MAPK regulated transcriptional activity as shown here for ELK-1, which is associated with proliferative activity of gynecological tumors [26,27].

The IRS-1/IRS-2 pathway and downstream components controlled by MT19c are primarily linked to IGF1R and IR signaling and can be inhibited by TNFR signaling as well. MT19c led to strong activation of SAPK/JNK, which mediates IRS-1 and IRS-2 inhibition as a downstream executor of TNFR signaling [28]. In summary, the data support the finding that MT19c cytotoxicity (Fig. 6D) is at least partially mediated by directly suppressing the IRS-1/2 pathway and downstream factors as well as by TNFR associated signaling via SAPK/JNK activation which in turn suppresses IRS-1/2 function [29].

The induction of apoptosis by MT19c on various levels such as caspase activation, DNA-fragmentation, is likely linked to the modulation of the IRS-1/2 pathway. This hypothesis is supported by findings that cells over-expressing IRS-1 and -2 resist apoptotic triggers [30]. Of particular interest for treatment with MT19c is the fact that IRS-1 is constitutively phosphorylated and expressed highly in primary malignant EOC tissues [20]. The cytotoxic activity of MT19c is complemented by an antiproliferative effect observed at sub-cytotoxic concentrations and by G1-phase accumulation via regulation of cell-cycle regulators p16, p21 cyclin-D1 and -D3. This effect may be partially linked to IRS-1 signaling because IRS-1 (but not IRS-2) reconstituted cell cycle progression in IRS-1 null cell lines [20]. Cyclin-D1, -D3, p16 and p21 are key regulators during G1/S cell cycle progression in cancer cells [29]. Targeting cell cycle regulators as well as with IRS-1 signaling, as achieved by MT19c, is a potent strategy to treat EOC [21,31].

Finally, to evaluate the *in vivo* efficacy of MT19c in epithelial ovarian cancer and gain insight into MT19c regulated pathways/targets, we conducted a SKOV-3 ovarian cancer xenograft study and analyzed MT19c modulated pathways by a Gene Set Enrichment Analysis (GSEA) of genomewide mRNA of the naïve and drug treated tumors [32]. MT19c treatment significantly suppressed the progression of the tumor growth within 35 days of study. GSEA analysis of the drug treated tumors showed that energy metabolism genes including transcripts coding for oxidative phosphorylation machinery were down-regulated by MT19c compared to naïve tumors. On the other hand, genes involved in double strand break repair (XRCC4, RAD54B and RAD50), protein turnover, and apoptosis were enriched in MT19c treated tumors.

In conclusion, we present a new approach to the design vitamin-D derivatives such as MT19c, which are devoid of the classic vitamin-D toxicities. MT19c, the first true non-hypercalcemic vitamin-D derivative, reveals promising anti-cancer activities in various *in vitro* and *in vivo* ovarian cancer model and demonstrated a lack of hypercalcemia in animals during the course of 90 days of treatment with 5 mg/kg bwt MT19c.

Conflict of interest statement

RKS and LB are co-applicants for a pending patent application. Other authors declare no conflict of interest.

Acknowledgments

This research was supported, in part, by a grant from 'Swim Across America' fund to RKS and RGM. Authors thank NIH COBRE Grant 1-P2ORR018728 for providing instrumentation support.

Appendix A. Supplementary data

Supplementary data to this article can be found online at doi:10.1016/j.ygyno.2011.07.002.

References

- [1] Lamberth E, Gregory WM, Nelstrop AE, Rustin GL. Long-term survival in 463 women treated with platinum analogs for advanced epithelial carcinoma of the ovary: life expectancy compared to women of an age-matched normal population. *Int J Gynecol Cancer* 2004;14:772–8.
- [2] Piccart MJ, Bertelsen K, James K, Cassidy J, Mangioni C, Simonsen E, et al. Randomized intergroup trial of cisplatin-paclitaxel versus cisplatin-cyclophosphamide in women with advanced epithelial EOC: three-year results. *J Natl Cancer Inst* 2000;92:699–708.
- [3] Deeb KK, Trump DL, Johnson CS. Vitamin-D signaling pathways in -cancer: potential for anti-cancer therapeutics. *Nat Rev Cancer* 2007;7:684–700.
- [4] Beer TM, Myrthue A, Calcitriol in cancer treatment: from the lab to the clinic. *Mol Cancer Ther* 2004;3:373–83.
- [5] Mantell DJ, Owens PE, Bundred NJ, Mawer EB, Canfield AE. 1 α ,25-dihydroxyvitamin D3 inhibits angiogenesis *in vitro* and *in vivo*. *Circ Res* 2000;87:214–20.
- [6] Brard L, Kalkunte S, Singh RK. Heterocycles and derivatives thereof and methods of manufacture and therapeutic use. WO/2007/070494.
- [7] Singh RK, Lange TS, Kim KK, Singh AP, Vorsa N, Brard L. Isothiocyanate NB7M causes selective cytotoxicity, pro-apoptotic signaling and cell-cycle regression in ovarian cancer cells. *Br J Cancer* 2008;99:1823–31.
- [8] Teichert A, Arnold LA, Otiemo S, Oda Y, Augustinaite I, Geistlinger TR, et al. Quantification of the vitamin D receptor–coregulator interaction. *Biochemistry* 2009;48:1454–61.
- [9] Guyton KZ, Kensler TW, Posner GH. Vitamin D and vitamin D analogs as cancer chemopreventive agents. *Nutr Rev* 2003;61:227–38.
- [10] Srivastava MD, Ambrus JL, Uskokovic MR. Calcitriol analogs cause differentiation of neoplastic cells in culture. *Res. Comm Mol Pathol Pharmacol* 1995;88:79–85.
- [11] Gobeil S, Boucherb CC, Nadeau D, Poirier GG. Characterization of the necrotic cleavage of poly(ADP-ribose) polymerase (PARP-1): implication of lysosomal proteases. *Cell Death and Diff* 2001;8:588–94.
- [12] Johnson DG, Walker CL. Cyclins and cell cycle checkpoints. *Ann Rev Pharmacol Toxicol* 1999;39:295–312.
- [13] Goettlieb WH, Bruchim I, Gu J, Shi Y, Camirand A, et al. Insulin-like growth-factor receptor-1 targeting in epithelial EOC. *Gynecol Oncol* 2006;100:389–96.
- [14] Akutsu N, Lin R, Bastien Y, Bestawros A, Enepekides DJ, et al. Regulation of gene expression by 1 α ,25-hydroxyvitamin D3 and its analog EB1089 under growth-inhibitory conditions in squamous carcinoma cells. *Mol Endocrinol* 2001;15:1127–39.
- [15] Takahashi F, Finch JL, Denda M, Dusso AS, Brown AJ, et al. A new analog of 1,25-(OH)₂D₃, 19-NOR,1,25-(OH)₂D₂, suppresses serum PTH and parathyroid gland growth in uremic rats without elevation of intestinal vitamin D receptor content. *Am J Kidney Dis* 1997;30:105–12.
- [16] Peleg S, Ismail A, Uskokovic MR, Avnur Z. Evidence for tissue- and cell-type selective activation of the vitamin D receptor by Ro-26-9228, a noncalcemic analog of vitamin D₃. *J Cell Biochem* 2003;88:267–73.
- [17] Brown AJ, Finch JL, Takahashi F, Slatopolsky EC. Calcemic activity of 19-Nor-1,25-(OH)₂D₂ decreases with duration of treatment. *J Am Soc Nephrol* 2000;11:2088–94.
- [18] Rozen F, Pollak MA. Inhibition of insulin-like growth-factor-1 receptor signaling by the vitamin D analogue EB1089 in MCF-7 breast -cancer cells: role for insulin-like growth-factor binding proteins. *Int J Oncol* 1999;15:589–94.
- [19] Ravikumar S, Perez-Liz G, Del Vale L, Soprano DR, Soprano KJ. Insulin-receptor Substrate-1 is an important mediator of EOC cell-growth suppression by all-trans retinoic acid. *Cancer Res* 2007;67:9266–75.
- [20] Wick KR, Werner ED, Langlais P, Ramos FJ, Dong LQ, et al. Grb10 inhibits insulin-stimulated insulin-receptor substrate (IRS)-phosphatidylinositol 3-kinase/Akt signaling pathway by disrupting the association of IRS-1/IRS-2 with the insulin-receptor. *J Biol Chem* 2003;278:8460–7.
- [21] Dearth RK, Cui X, Kim HJ, Hadsell DL, Lee AV. Oncogenic transformation by the signaling adaptor proteins insulin-receptor substrate (IRS)-1 and IRS-2. *Cell Cycle* 2007;6:705–13.
- [22] Mardilovich K, Pankratz SL, Shaw LM. Expression and function of the insulin-receptor substrate proteins in cancer. *Cell Commun Sig* 2009;7:14–28.
- [23] Smith JA, Poteet-Smith CE, Xu Y, Errington TM, Hecht SM, et al. Identification of the first specific inhibitor of p90 ribosomal-S6 kinase (RSK) reveals an unexpected role for RSK in cancer cell-proliferation. *Cancer Res* 2005;65:1027–34.
- [24] McPhillips F, Mullen P, MacLeod KG, Sewell JM, Monia BP, et al. Raf-1 is the predominant Raf isoform that mediates growth-factor-stimulated growth in EOC cells. *Carcinogenesis* 2006;27:729–39.

- [25] MacKeigan JP, Collins TS, Ting JPY. MEK inhibition enhances paclitaxel-induced tumor apoptosis. *J Biol Chem* 2000;275:38953–6.
- [26] Uht RM, Amos S, Martin PM, Riggan AE, Hussaini IM. The protein kinase C-beta isoform induces proliferation in glioblastoma cell-lines through an ERK/Elk-1 pathway. *Oncogene* 2007;26:2885–93.
- [27] Maniccia AW, Lewis C, Begum N, Xu J, Cui J, et al. Mitochondrial localization, ELK-1 transcriptional regulation and growth inhibitory functions of BRCA1, BRCA1a, and BRCA1b proteins. *J Cell Physiol* 2009;219:634–41.
- [28] Grounds MD, Radley HG, GebSKI BL, Bogoyevitch MA, Shavlakadze T. Implications of cross-talk between tumour necrosis factor and insulin-like growth-factor-1 signaling in skeletal muscle. *Clin Exp Pharmacol Physiol* 2008;35:846–51.
- [29] Bruning JC, Winnay J, Cheatham B, Kahn CR. Differential signaling by insulin-receptor substrate 1 (IRS-1) and IRS-2 in IRS-1-deficient cells. *Mol Cell Biol* 1997;17:1513–21.
- [30] Uchida T, Myers Jr MG, White MF. IRS-4 mediates protein kinase B signaling during insulin stimulation without promoting anti-apoptosis. *Mol Cell Biol* 2000;20:126–38.
- [31] Andrilli GD, Kumar C, Scambia G, Giordano A. Cell cycle genes in EOC: step toward earlier diagnosis and novel therapies. *Clin Cancer Res* 2004;10:81132–41.
- [32] Stuckey A, Fischer A, Miller DH, Hillenmeyer S, Kim KK, Ritz A, Singh RK, Raphael BJ, Brard L, and Brodsky AS. Integrated genomics of ovarian xenograft tumor progression and chemotherapy response. *BMC Cancer* in press, doi:10.1186/1471-2407-11-308.